Progressive Failure Analysis of Plain Weaves Using Damage Mechanics Based Constitutive Laws

M. Kollegal, S. N. Chatterjee and G. Flanagan
Materials Sciences Corporation,
500 Office Center Drive, Suite 250
Fort Washington, PA 19034

The behavior of plain woven fabric composites is studied using three-dimensional finite elements which allows detailed modeling of the geometric complexities and spatial material variations within the fabric. Damages in the composite constituents viz. yarn and pure matrix are modeled on a continuum basis and related to their material constitutive behavior. The 3D constitutive laws describing pure matrix and yarn behavior are developed using a damage mechanics based approach with the dissipated energy density as the damage parameter. The strain energy dissipation (SED) concept is employed to describe the damage state and current stiffnesses of the weave constituents. A progressive failure analysis of plain woven fabrics subjected to tension and in-plane shear is carried out considering both geometric and material nonlinearities. The initiation and progression of damage within the fabric is investigated and the significant damage mechanisms outlined.

Keywords: Woven composites, finite element analysis, damage mechanics, constitutive laws, failure

INTRODUCTION

Micromechanics of textile composites has been the focus of study by many investigators [1-11]. The proper description of the internal weave geometry and spatial variation in material properties within the fabric presents a formidable task in the analysis of such composites. Most of the analytical studies on such composites have focussed on predicting their elastic properties [1-7]. Studies relating to prediction of their strength and failure modes are relatively few [8-11].

A detailed study of the significant stresses and strains developed within the fabric and possible damage mechanisms can be accomplished by the use of three-dimensional finite elements. Nonlinear material behavior of composites is due to damage accumulation, which causes changes in the stiffnesses of the material. It is well known that macroscopic failure is preceded by an accumulation of different types of microscopic damage and stiffness losses due to the accumulation of such damage, which cause significant load

Report Documentation Page

Form Approved
OMB No. 0704-0188

1. REPORT DATE	2. REPORT TYPE	3. DATES COVERED
2006		**00-00-2006 to 00-00-2006**

4. TITLE AND SUBTITLE	5a. CONTRACT NUMBER
Progressive Failure Analysis of Plain Weaves Using Damage Mechanics Based Constitutive Laws	5b. GRANT NUMBER
	5c. PROGRAM ELEMENT NUMBER
6. AUTHOR(S)	5d. PROJECT NUMBER
	5e. TASK NUMBER
	5f. WORK UNIT NUMBER
7. PERFORMING ORGANIZATION NAME(S) AND ADDRESS(ES) **Materials Science Corporation,500 Office Center Drive Suite 250,Fort Washington,PA,19034**	8. PERFORMING ORGANIZATION REPORT NUMBER
9. SPONSORING/MONITORING AGENCY NAME(S) AND ADDRESS(ES)	10. SPONSOR/MONITOR'S ACRONYM(S)
	11. SPONSOR/MONITOR'S REPORT NUMBER(S)

12. DISTRIBUTION/AVAILABILITY STATEMENT
Approved for public release; distribution unlimited

13. SUPPLEMENTARY NOTES
The original document contains color images.

14. ABSTRACT

15. SUBJECT TERMS

16. SECURITY CLASSIFICATION OF:			17. LIMITATION OF ABSTRACT	18. NUMBER OF PAGES	19a. NAME OF RESPONSIBLE PERSON
a. REPORT	b. ABSTRACT	c. THIS PAGE			
unclassified	**unclassified**	**unclassified**		**24**	

redistribution. Final failure usually occurs due to the development of one or more areas of highly localized stiffness losses, which behave as macroscopic damages or cracks. Hence, a proper modeling of the damage growth, stiffness loss and load redistribution is essential for a reliable prediction of the weave response.

Existing FE modeling tools and preprocessors are not adequate for rapidly creating complex 3-dimensional models needed for the purpose. Therefore, mesh generation programs were developed which would easily interface with a general purpose FEA software, ABAQUS [12]. FE models can be generated for plain weaves and higher-order satin-weaves using a minimal definition of the textile architecture. In the present approach, damages in the composite constituents are modeled on a continuum basis and related to the material constitutive behavior. The 3D constitutive laws describing matrix and yarn behavior are developed using a damage mechanics based approach, with the dissipated energy density as the damage parameter. The strain energy dissipation (SED) concept is employed to describe the damage state and current stiffnesses of the weave constituents. The yarns are treated as transversely isotropic while the pure matrix pockets are assumed to be isotropic.

The developed methodology for geometric and damage modeling in fabric composites is demonstrated through an investigation of progressive failure of plain woven composites subjected to external loads. Two loading conditions are considered viz. in-plane tension and in-plane shear. For a realistic modeling of the weave response, both geometric and material nonlinearities are considered. The inititiation and growth of damage within the fabric is investigated and the important stresses causing failure identified.

GEOMETRIC MODELING

In the current analysis, the yarns follow a specified path that combines flat segments with sinusoidal undulations where orthogonal yarns cross. The yarn path and cross-sectional geometry of the yarns are similar to that described in Ref. [3]. The cross-section profile of the yarns and the undulation path can be

described in terms of yarn width, filament count and fiber volume fraction. They provide an adequate representation of the varying cross-sectional profile and undulation of the yarns.

The periodic nature of the yarn undulations makes it possible to identify repetitive portion of the woven fabric. The mechanical response of the fabric can then be described by analyzing such repetitive portions, termed as *unit cell*, of the textile. The *unit cell* with appropriate boundary conditions can thus be used to examine the behavior of the entire textile subjected to various loading conditions. Unit cells of the textile forms considered in the present study are shown in Fig. 1.

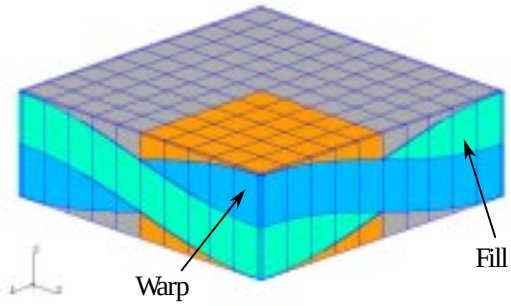

(a)

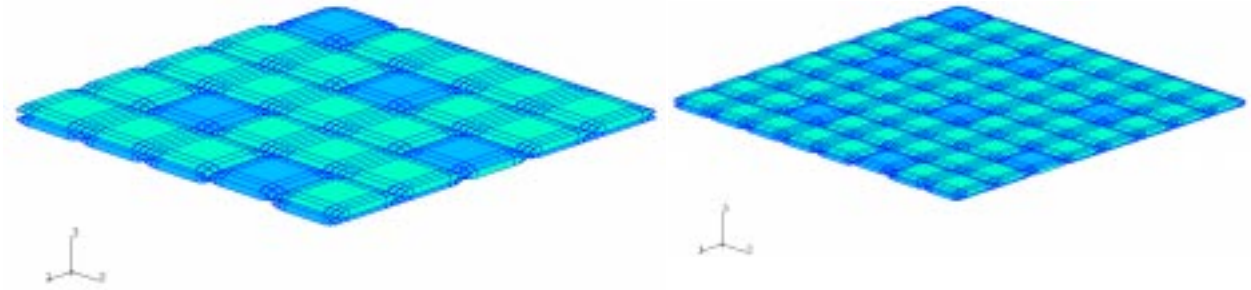

(b) (c)

Figure 1: (a) Plain Weave (one quarter highlighted) (b) 5 harness satin (c) 8 harness satin

FINITE ELEMENT DISCRETIZATION

The weaves are discretized employing 20 noded, 15 noded and 10 noded three-dimensional elements and the resulting mesh analyzed using ABAQUS [12]. An in-house, parametric finite element mesh gen-

erator which permits an automatic meshing of the weave unit cell and ABAQUS input file generation is used for this purpose. For the case of plain weaves, the point symmetrical material distribution about the *z*-axis within the unit cell (Fig. 1a) makes it possible to analyze only one quarter (Figure 2) with appropriate boundary conditions. This results in a reduction of the problem size and computational time.

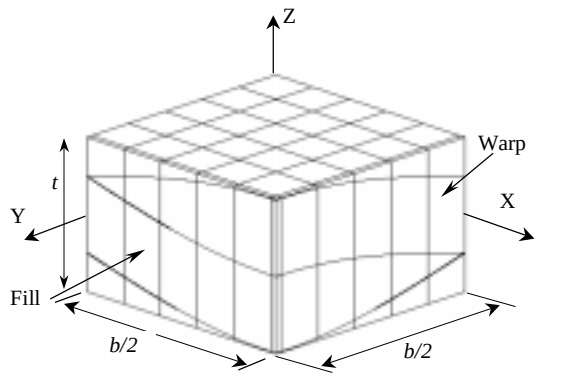

Figure 2 Quarter Cell of Plain Weave

Details of the displacement boundary conditions applicable to the quarter cell single layer plain weave model (Figure 2) are described in Ref. [13] and are summarized below. The surfaces z = ±*t*/2 are assumed to be stress free.

For the case of inplane extensional loading in the *x* direction:

$$
\begin{aligned}
&On\,the\ plane\ x = 0\ :\quad u(0,y,z) = -u(0,y,-z)\\
&\qquad\qquad\qquad\qquad\ v(0,y,z) = v(0,y,-z)\\
&\qquad\qquad\qquad\qquad\ w(0,y,z) = -w(0,y,-z)\\
&On\,the\ plane\ y = 0\ :\quad u(x,0,z) = u(x,0,-z)\\
&\qquad\qquad\qquad\qquad\ v(x,0,z) = -v(x,0,-z)\\
&\qquad\qquad\qquad\qquad\ w(x,0,z) = -w(x,0,-z)\\
&Along\ \ the\ z-axis\ \ (0,0,z)\ :\quad u(0,0,z) = 0\\
&\qquad\qquad\qquad\qquad\ v(0,0,z) = 0\\
&\qquad\qquad\qquad\qquad\ w(0,0,z) = -w(0,0,-z)
\end{aligned}
\tag{1}
$$

$$On\ the\ plane\ x = b/2: \quad u(\frac{b}{2},y,z) = \frac{u_0}{2}$$

$$On\ the\ plane\ y = b/2: \quad v(x,\frac{b}{2},z) = \frac{v_0}{2}$$

u_o / b and v_o / b are average extensional strains in *x* and *y* directions, respectively. No shear tractions are applied at x = *b*/2 and y = *b*/2.

The boundary conditions for inplane shear loading are:

$$\begin{aligned}
On\ the\ plane\ x = 0 \quad & u(0,y,z) = u(0,y,-z) \\
& v(0,y,z) = -v(0,y,-z) \\
& w(0,y,z) = w(0,y,-z) \\
On\ the\ plane\ y = 0 \quad & u(x,0,z) = -u(x,0,-z) \\
& v(x,0,z) = v(x,0,-z) \\
& w(x,0,z) = w(x,0,-z) \\
On\ the\ plane\ y = \frac{b}{2} \quad & u(x,\frac{b}{2},z) = \frac{p}{2} \\
& w(x,\frac{b}{2},z) = 0 \\
On\ the\ plane\ x = \frac{b}{2} \quad & v(\frac{b}{2},y,z) = \frac{p}{2} \\
& w(\frac{b}{2},y,z) = 0
\end{aligned} \tag{2}$$

p/*b* is the average in-plane shear strain. No shear traction in *z*-direction and extensional stresses at x = b/2 and y = b/2 are applied. It should be noted that for a multilayer fabric composite the surfaces of each layer can not be assumed to be stress-free. The single layer model discussed above yields an approximate measure of the in-plane stiffnesses of a multilayered composite and the stresses in the boundary layers.

ELASTIC ANALYSIS

In order to validate the weave finite element models, the elastic properties of plain, 5-harness satin and 8 - harness weaves are first computed. The present values are compared against analytical and experimental results available in literature. AS4 Graphite/Epoxy 3501 woven fabrics [3] having a yarn fiber volume

fraction of 0.75 are selected for the purpose. The width of the yarns was 1.411 mm and its thickness was 0.01 mm. The filament count in both the warp and fill tows was assumed to be 3000 [3]. The material properties of AS4-Graphite/epoxy yarns and matrix are shown in Table 1. Table 2 shows a comparison of the current results with other analytical and experimental results for plain, 5-harness and 8-harness satin weaves. For an AS4 graphite/epoxy cross-ply laminate having an overall fiber volume fraction equal to that of the fore mentioned weaves (V_f = 0.64), the elastic modulus computed using the Classical Lamination Theory is 67.60 GPa [3]. It can be seen that the undulation of the yarns causes a reduction in the inplane extensional stiffness of the weaves and this reduction is maximum in plain weaves where the effect of yarn cross-over is maximum.

MATERIAL MODELING

The nonlinear behavior of the weave constituents viz. yarns and pure matrix is modeled using a damage mechanics approach. Constitutive laws for continuum damage mechanics are discussed in Ref. [14-17]. Such models have been found to be successful in representing the behavior of brittle materials. They make use of a phenomenological approach and damage variables such as average crack densities. In the present study, the dissipated energy density (ϕ) is chosen as the damage parameter. The nature of a damage surface for a fixed value of ϕ and its change with ϕ can be modeled at various levels of complexity to simulate the "in-situ" nonlinear material behaviors. Details of the constitutive modeling of the yarns and pure matrix are shown in Appendix A. Simple quadratic forms of the damage surfaces in terms of chosen strain variables are employed. The changes of these surfaces with ϕ are chosen in a manner such that they yield power law type stress-strain relations under unidirectional straining beyond the initial elastic domain.

The material constitutive laws for yarns and pure matrix are incorporated as a user subroutine in ABAQUS [12]. The material properties required for analyses are the elastic moduli, Poisson's ratios and

the variables that describe the damage surfaces in the strain space for various values of dissipated energy density ϕ in the yarn/matrix.

NONLINEAR ANALYSIS

A typical unit cell of a plain weave discretized by finite elements is shown in Figure 1a. Within each finite element of the unit cell, the stiffnesses, stresses and strains can be monitored at the material integration points. This function is performed by the material models described in the Appendix. For this purpose, the constitutive laws for the materials are implemented through a user-defined subroutine (UMAT) and linked with the finite element analysis program, ABAQUS. During each load increment of the nonlinear analysis process, the material definition routines describe the current stiffnesses and damage state at the numerical integration points of the finite elements. The reductions in stiffnesses occurring as a result of localized damage within the yarn/pure matrix pockets are monitored and incorporated into the weave response.

An incremental-iterative approach is adopted for the nonlinear finite element analysis. The modified Newton-Raphson method is used to trace the loading path of the structure. The nonlinear analysis starts from an equilibrium state. Loads are applied by prescribing incremental displacements and the unbalanced forces evaluated. An iterative procedure is used until the out-of-balance load vector or the displacement increments are sufficiently small. Within each element representing yarn/pure matrix, each Gaussian integration point represents a certain volume of material whose material stiffnesses are described by the user material definition subroutine developed. Within each load increment of the nonlinear analysis, the material is checked for occurrence of damage. Once damage is detected, the material properties are changed accordingly.

The behavior of balanced E-Glass/epoxy [9] and AS4-Carbon/epoxy [8] and Carbon/epoxy [6] plain woven fabric, described earlier, when subjected to in-plane loads is examined. The current predictions are compared with experimental results if available or with other theoretical results available in literature. Elastic properties of the weave constituents are tabulated in Table 1. The geometrical parameters of the weave used in the present investigation are listed in Table 3.

Tensile Behavior

The plain woven fabrics are subjected to tensile loading along warp using boundary conditions described in Eqn. 1. Effects of geometric nonlinearity and material nonlinearity of the yarns and surrounding pure matrix are included in the analysis. Figures 3 and 4 show the stress/strain curves obtained from the present FEA.

These results are compared with experimental values [6, 8, 9]. Figure 3 shows a good agreement between the results of the present analysis and experimental values in the pre-'knee' portion of the stress-strain curve. The 'knee' in the stress-strain curve is caused due to transverse tensile failure in the fill. Unlike E-Glass/epoxy plain weave, in AS4-Carbon/epoxy plain weave (Figure 4) the intermediate damage mechanisms (e.g. 'knee') are not seen clearly in the stress/strain response prior to final failure of the weave, i.e. the stress/strain plot is almost linear until final failure. In the case of E-Glass/epoxy plain weave, the 'knee' is more pronounced than that in AS4-Carbon/epoxy plain weave. The damage mechanisms seen in the plain weaves subjected to tension along warp direction are: (i) Transverse tensile failure (of matrix) in fill. (ii) Axial shear failure of the fill near the yarn extremities where there is a stress concentration and (iii) Fiber tensile failure in the warp.

Figure 5 shows the behavior of Carbon/epoxy plain weave lamina [6] subjected to tension along warp and tension along an off-axis ($\theta = 15^{o}$) direction. In off-axis tensile loading, the boundary conditions

for inplane extensional case induce shearing deformations within the unit cell apart from extensional actions. For the case of off-axis loading, considerable shear softening occurs in the transverse fill before final failure of the weave. Damage in the fill due to transverse tension occurs much earlier (177 MPa) than the damage in the warp caused by fiber failure. The damage mechanisms seen in the plain weave subjected to off-axis tension are: (i) Transverse tensile failure (of matrix) in fill. (ii) Axial shear failure in fill and (iii) Fiber failure in tension in warp.

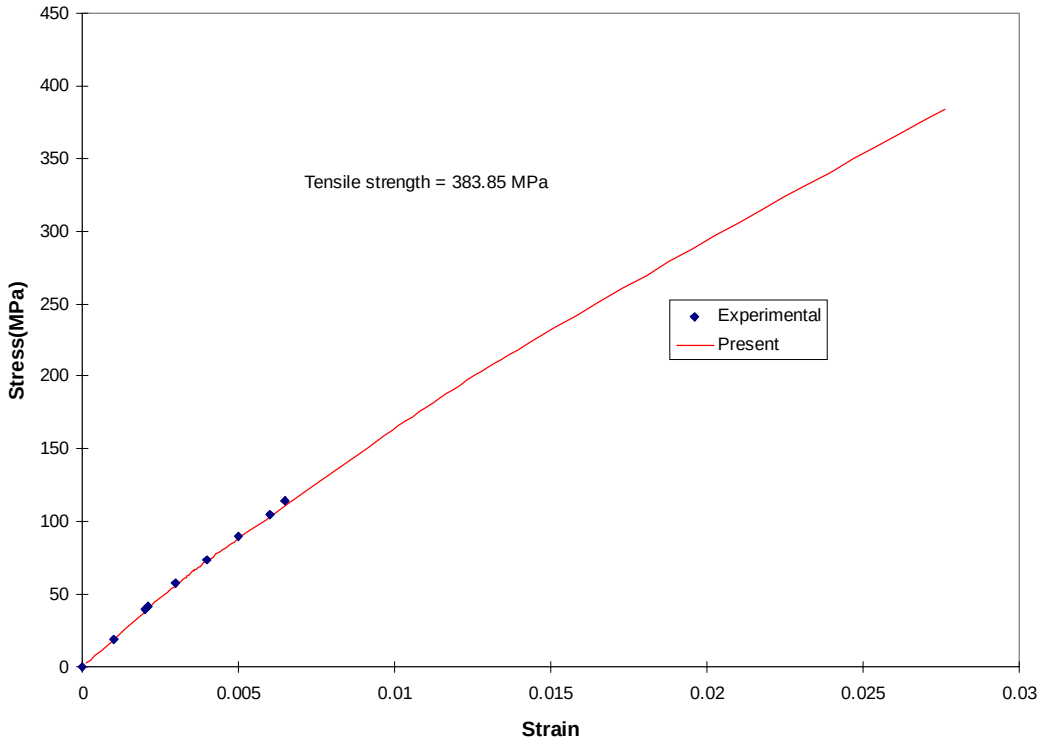

Figure 3 Response of E-Glass/Epoxy Plain Weave Subjected to Tension

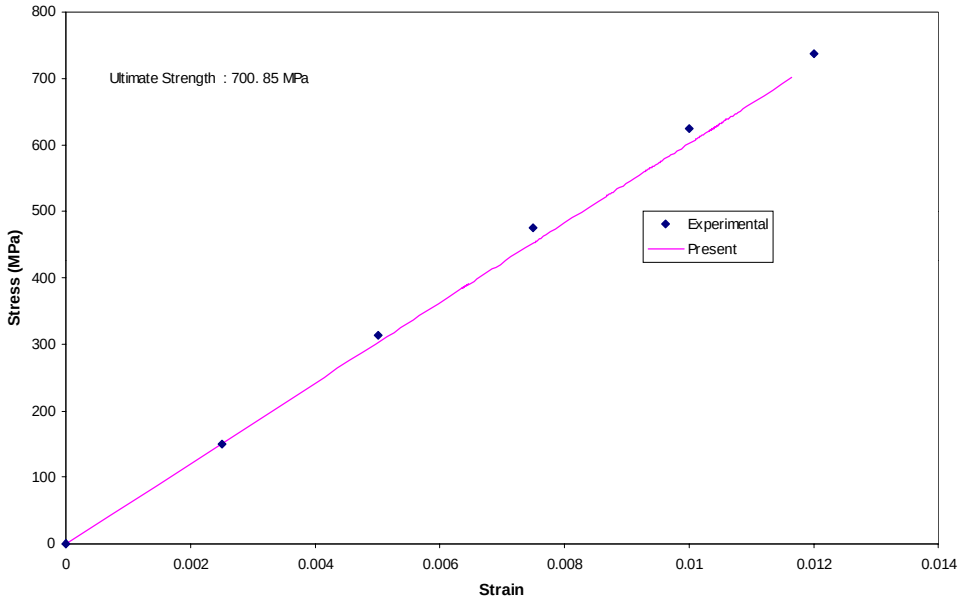

Figure 4. Response of AS4/Carbon/Epoxy Plain Weave Subjected to Tension

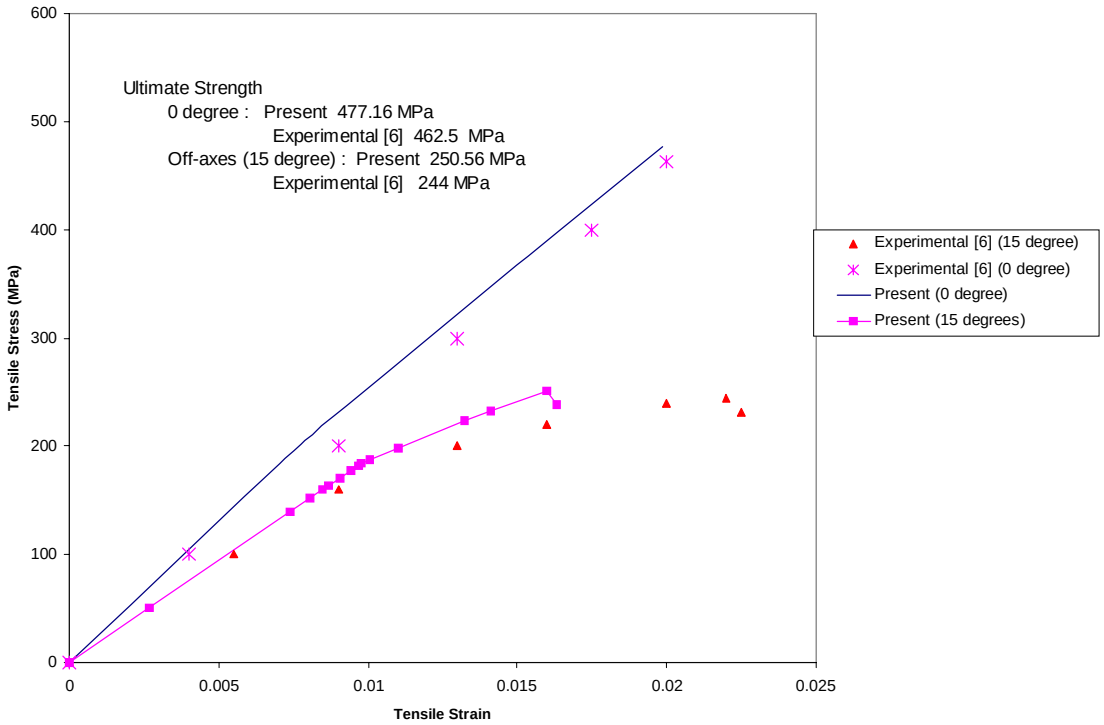

Figure 5: Response of Carbon/epoxy [6] plain weave subjected to on-axis and off-axis tension

In-Plane Shear

The behavior of E-Glass/epoxy and AS4-Carbon/epoxy plain weaves under in-plane shear is examined using boundary conditions shown in Eqn. 2. Figures 6 and 7 show the stress-strain curves obtained from the present analysis. For the case of AS4-Carbon/epoxy plain weave, the present results are compared with an experimental result available in literature [8]. The ultimate strength prediction agrees well with the experimental result though the failure strains differ. This could be due to differences in material properties used in the present material model and those tested. The sequence of failure for plain weaves subjected to inplane shear is (i) Axial shear failure in fill (ii) Transverse shear failure in warp (iii) matrix failure in transverse tension in fill.

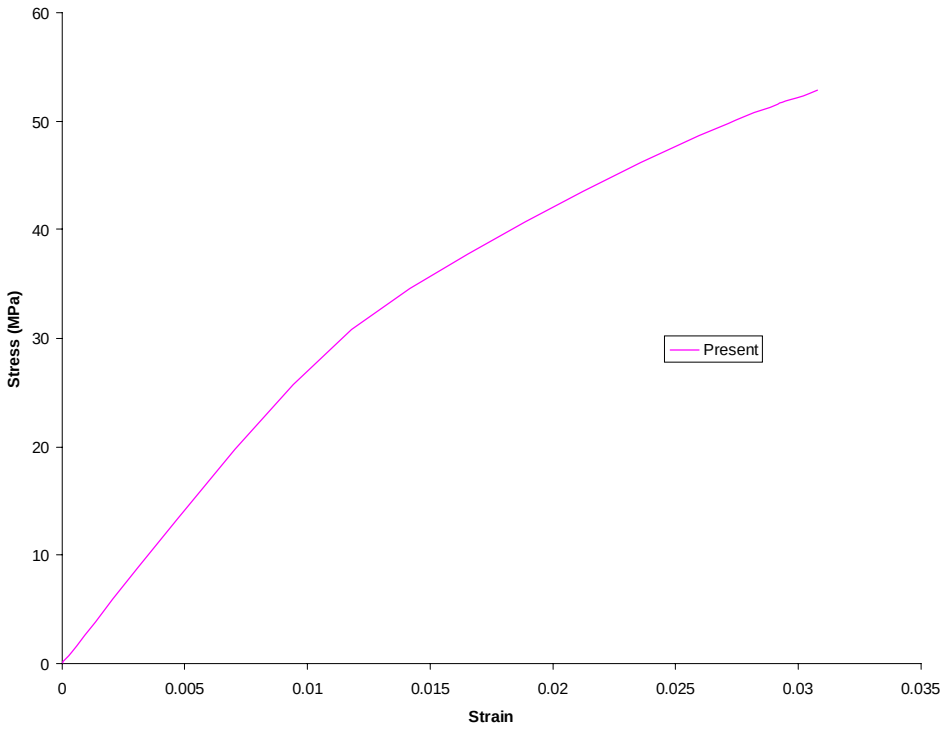

Figure 6. Response of E-Glass/Epoxy Plain Weave Subjected to Inplane Shear

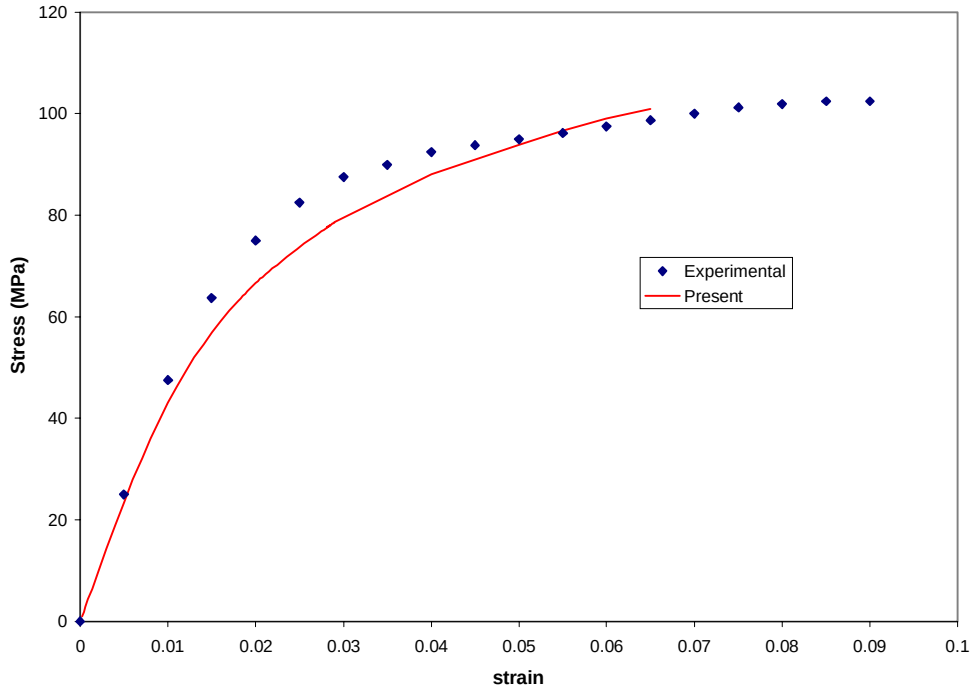

Figure 7. Response of AS4-Carbon/Epoxy Plain Weave Subjected to In-Plane Shear

CONCLUSIONS

An investigation into the micromechanics of fabric composites has been attempted using 3D finite elements and a damage mechanics based constitutive model for the yarns and pure matrix. The strain energy dissipation ϕ is chosen as the damage parameter and the nature of damage surface for a particular value of ϕ and its change with ϕ modeled. In the present study, simple quadratic forms of the damage surfaces in terms of chosen strain variables are used to simulate the "in-situ" nonlinear material behavior. The changes of these surfaces with ϕ are chosen in a manner such that they yield power law type stress-strain relations under unidirectional straining beyond the initial elastic domain. The material model has been used to study and describe the initiation and growth of damage in plain woven fabrics. A progressive failure analysis of plain woven fabrics subjected to inplane loading has been undertaken and the results compared with analytical/experimental results in literature. Plain weaves, when subjected to tension exhibit an almost linear

behavior prior to failure. The dominant failure mechanism is transverse tensile failure of the fill for a plain weave loaded in the warp direction. Such failure causes a reduction in the stiffness of the plain weave and is reflected as a "knee" in the stress-strain plot. Plain woven fabrics exhibit a non-linear behavior when subjected to inplane shear. This nonlinear behavior is mainly due to the shear softening of matrix in the yarns. Failure of matrix in warp due to inplane shear and transverse tensile failure of the fill are prime mechanisms of failure under such loading conditions.

ACKNOWLEDGEMENTS

Support for this work by the Air Force Office of Scientific Research under Contract No. F49620-96-C-0018 is gratefully acknowledged.

REFERENCES

[1] Chou, T. W. 1992. Microstructural Design of Fiber Composites. Cambridge University Press, Cambridge, UK.

[2] Dow, N. F., Ramnath, V and Rosen, B. W. 1987. Analysis of Woven Fabrics for Reinforced Composite Materials, NASA-CR-178275, NASA, Hampton, Virginia.

[3] Naik, R. A. 1994. Analysis of Woven and Braided Fabric Reinforced Composites, NASA CR 194930, NASA, Hampton, Virginia.

[4] Kuhn, J. L and Charalambides, P. G. 1998. Elastic Response of Porous Matrix Plain Weave Fabric Composites: Part I-Modeling. Journal of Composite Materials, Vol. 32, No. 16, pp. 1426-1471.

[5] Kuhn, J. L and Charalambides, P. G. 1998. Elastic Response of Porous Matrix Plain Weave Fabric Composites: Part II-Results. Journal of Composite Materials, Vol. 32, No. 16, pp. 1472-1508.

[6] Naik, N. K. 1994. Woven Fabric Composites, Technomic Pub. Co., Lancaster, PA.

[7] Whitcomb, J. D. 1989. Three-dimensional Stress Analysis of Plain Weave Composites. Paper presented at the 3rd Symposium of Composite Materials: Fatigue and Fracture, Orlando, Florida, October 1989. ASTM STP n 1110, 1991.

[8] Blackketter, D. M., Walrath, D. E., and Hansen, A. C., 1993. Modeling Damage in a Plain Weave Fabric-Reinforced Composite Material. Journal of Composites Technology and Research, 15, No. 2, pp. 136-142.

[9] Dasgupta A. and Bhandarkar S. M. 1994. Effective Thermomechanical Behavior of Plain-Weave Fabric Reinforced Composites Using Homogenization Theory. Journal of Engineering Materials and Technology, Transactions of the ASME, 116, pp. 99-105.

[10] Makoto, I. and Chou, T. W. 1998. An Analytical and Experimental Study of Strength and Failure Behavior of Plain Weave Composites. Journal of Composite Materials, Vol. 32, No. 1, pp. 2-30.

[11] Naik, A. R. 1994. Failure Analysis of Woven and Braided Fabric Reinforced Composites. NASA-CR-194981, NASA, Hampton, Virginia.

[12] ABAQUS, ver 5.7, Hibbitt, Karlsson & Sorensen, Inc., Pawtucket, RI.

[13] Flanagan, G., S. Chatterjee and M. Kollegal 1999. Stress Analysis and Damage Modeling of Textile Composites. MSC TFR 3909/DA09, Submitted to Air Force Office of Scientific Research, Bolling AFB, DC.

[14] Krajcinovic, D. 1985. Continuous Damage Mechanics Revisited - Basic Concepts and Definitions. ASME J. Appl. Mech., Vol. 52, p. 829.

[15] Illankamban, R., and Krajcinovic, D. 1987. A Constitutive Theory for Progressively Deteriorating Solids. International Journal of Solids and Structures, Vol. 23, p. 1521.

[16] Chaboche, J.L. 1989. Continuum Damage Mechanics, Parts I and II. ASME J. Applied Mechanics, Vol. 55, p. 59 and p. 65.

[17] Mast, P.W. et al. 1995. Characterization of Strain-Induced Damage in Composites Based on the Dissipated Energy Density, Parts I-III. Theoretical and Applied Fracture Mechanics, Vol. 22, p. 71, p. 97, p. 115.

[18] Chatterjee, S. N. 1999. Damage, Stiffness Loss and Failure in Composite Structures, ASTM Symposium on Composite Structures: Theory and Practice, to appear in ASTM STP 1383.

APPENDIX

Damage Mechanics Based Constitutive Laws

A continuum damage mechanics based model is used for representing the behavior of brittle materials. If internal damage variables be represented as ω^{α}, (such as average crack densities [15]), one can write the Clausius-Duhem inequality as

$$\underline{\sigma}\, d\underline{\varepsilon} - \rho d\psi = d\phi \geq 0; \tag{A1a}$$

where, $\underline{\sigma}$, $\underline{\varepsilon}$ are stress and strain vectors, respectively and ρ is the density

$\underline{\sigma} = \underline{\sigma}\,[\underline{\varepsilon}, \omega^{\alpha}; \alpha = 1, 2, \ldots k]$

k = total number of damage variables

$\psi = \psi\,[\underline{\varepsilon}, \omega^{\alpha}]$, Helmholtz free energy

$$\sigma_i = \rho \frac{\partial \psi}{\partial \varepsilon_i} \tag{A1b}$$

$\phi = \phi\,(\underline{\varepsilon}, \omega^{\alpha})$, the dissipated energy density

$$d\phi = \sum_{\alpha=1}^{k} R^{\alpha} d\omega^{\alpha} \geq 0 \tag{A1c}$$

R^{α} = conjugate thermodynamic force, an energy release rate for the

damage variable $\omega^{\alpha} = R^{\alpha}\,(\underline{\varepsilon}, \omega^{\alpha})$

$$= -\rho \frac{\partial \psi}{\partial \omega^{\alpha}} = \frac{\partial \phi}{\partial \omega^{\alpha}} \tag{A1d}$$

In the strain energy dissipation (SED) concept employed in [17], there is one damage variable (k = 1) which is the dissipated energy density ϕ ($=\omega^1$) and for this case one may choose the following form for the Helmholtz free energy

$$\rho\psi = \frac{1}{2} C_{ij} \varepsilon_i \varepsilon_j - \int_0^{\phi_c} R(\underline{\varepsilon}, \phi) d\phi \tag{A2}$$

where ϕ_c is the current value of ϕ and C_{ij} are the elastic stiffnesses in contracted notation. It follows from the expression for $R^1 = R$ in (A1d) then for damage growth to occur

$$R(\underline{\varepsilon}, \phi) = 1 \tag{A3}$$

which defines the damage surface (for a given value of ϕ) in the strain space and when $R(\underline{\varepsilon}, \phi) < 1$, no damage growth would occur. It is clear that the dissipated energy is a function of the strain variables independent of the loading path and unloading will occur in a straight line from the current strain state to the origin (Figure A1). Obviously, these assumptions have to be checked by conducting tests and it has been reported [17] that data justify these assumptions.

The damage surfaces have to be determined by suitable designed tests, so that in-situ behavior of the unidirectional composite or the matrix in a structure or a laminate can be modeled using these surfaces. A special test apparatus is described in [17] for determining the surfaces in a three-dimensional strain space (in-plane extensional and shear stresses) from tests on $(\pm\theta)_{ns}$ laminate specimens. Data from standard tensions and compression tests $(\pm\theta)_{ns}$ and $(0/90)_{ns}$ coupons as well as those from a quasi-isotropic laminate with a hole are used in [18] to obtain simple representations of damage surfaces in the same strain space. Such results are useful for modeling laminate behaviors. No representation of R in a six-dimensional strain space is reported in literature. Some simple forms are discussed next.

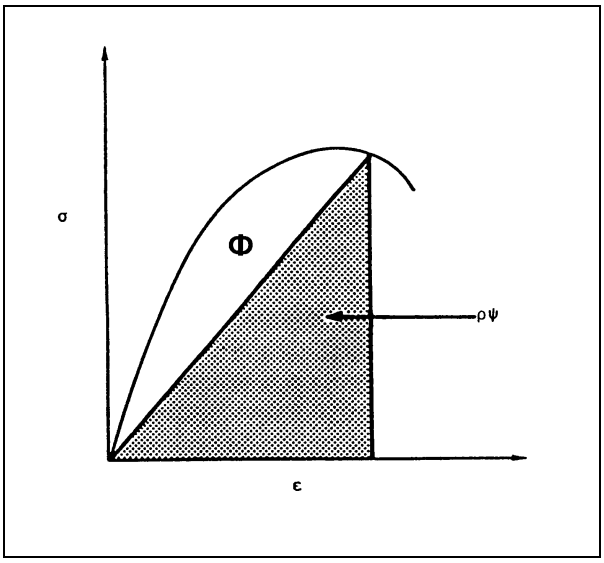

Figure A1. Helmholtz Free Energy and Dissipated Energy ϕ

DAMAGE SURFACES FOR TRANSVERSELY ISOTROPIC MATERIAL

For a fiber composite which is transversely isotropic in the elastic state, one can write the Helmholtz free energy in the following form.

$$\rho\psi = \frac{1}{2}\Big[C_{11}\varepsilon_1^2 + 2C_{12}\varepsilon_1\varepsilon_s + k\varepsilon_s^2 + G_T\left(\varepsilon_d^2 + \gamma_{23}^2\right) + G_A\left(\gamma_{12}^2 + \gamma_{13}^2\right)\Big] - \int_o^{\phi} R(\underline{\varepsilon},\phi)d\phi \qquad \text{(A4a)}$$

where

$$\varepsilon_s = \varepsilon_2 + \varepsilon_3$$
$$\varepsilon_d = \varepsilon_2 - \varepsilon_3 \qquad \text{(A4b,c)}$$

k is the plane strain bulk modulus and G_A and G_T are the axial and transverse shear moduli, respectively. The stresses are given by

$$
\begin{aligned}
\sigma_1 &= \frac{\partial(\rho\psi)}{\partial\varepsilon_1} \\
\frac{\sigma_2+\sigma_3}{2} &= \frac{\partial(\rho\psi)}{\partial\varepsilon_s} \\
\frac{\sigma_2-\sigma_3}{2} &= \frac{\partial(\rho\psi)}{\partial\varepsilon_d} \\
\tau_{12} &= \frac{\partial(\rho\psi)}{\partial\gamma_{12}} \\
\tau_{13} &= \frac{\partial(\rho\psi)}{\partial\gamma_{13}} \\
\tau_{23} &= \frac{\partial(\rho\psi)}{\partial\gamma_{23}}
\end{aligned}
\qquad \text{(A4d-i)}
$$

Based on the assumption of a quadratic interaction criterion in terms of stresses, one may choose the following form of R for zero (damage initiation) to moderate values of the dissipated energy density

$$
\begin{aligned}
\mathrm{R}(\underline{\varepsilon},\phi) = \frac{1}{2}\Big[&\left\{\mathrm{a}_{11}(\phi)+\mathrm{b}_{11}(\phi)\operatorname{sgn}\varepsilon_1^*\right\}\varepsilon_1^{*2} \\
&+\left\{\mathrm{a}_{22}(\phi)+\mathrm{b}_{22}(\phi)\operatorname{sgn}\varepsilon_s^*\right\}\varepsilon_s^{*2} \\
&+\mathrm{a}_{44}(\phi)\left(\varepsilon_d^2+\gamma_{23}^2\right)+\mathrm{a}_{66}(\phi)\left(\gamma_{12}^2+\gamma_{13}^2\right)\Big]
\end{aligned}
\qquad \text{(A5a)}
$$

where

$$
\begin{aligned}
\varepsilon_1^* &= \varepsilon_1+\alpha_{12}\varepsilon_s \\
\varepsilon_s^* &= \varepsilon_s+\alpha_{21}\varepsilon_1 \\
\alpha_{12} &= C_{12}/C_{11} \\
\alpha_{21} &= C_{12}/k
\end{aligned}
\qquad \text{(A5b-e)}
$$

Use of (A4a-i) yields a transversely isotropic material with the following values of reduced stiffnesses in the damaged state for the current value of ϕ.

$$
\begin{aligned}
\mathrm{C}_{11}^* &= \mathrm{C}_{11}-\left(\mathrm{A}_{11}(\phi)+\mathrm{B}_{11}(\phi)\operatorname{sgn}\varepsilon_1^*\right)-\left(\mathrm{A}_{22}(\phi)+\mathrm{B}_{22}(\phi)\operatorname{sgn}\varepsilon_s^*\right)\alpha_{21}^2 \\
\mathrm{C}_{12}^* &= \mathrm{C}_{12}-\left(\mathrm{A}_{11}(\phi)+\mathrm{B}_{11}(\phi)\operatorname{sgn}\varepsilon_1^*\right)\alpha_{12}-\left(\mathrm{A}_{22}(\phi)+\mathrm{B}_{22}(\phi)\operatorname{sgn}\varepsilon_s^*\right)\alpha_{21} \\
\mathrm{k}^* &= \mathrm{k}-\left(\mathrm{A}_{22}(\phi)+\mathrm{B}_{22}(\phi)\operatorname{sgn}\varepsilon_s^*\right)-\left(\mathrm{A}_{11}(\phi)+\mathrm{B}_{11}(\phi)\operatorname{sgn}\varepsilon_1^*\right)\alpha_{12}^2 \\
\mathrm{C}_{44}^* &= \mathrm{G}_T-\mathrm{A}_{44}(\phi) \\
\mathrm{C}_{66}^* &= \mathrm{G}_A-\mathrm{A}_{66}(\phi)
\end{aligned}
\qquad \text{(A5f-j)}
$$

where

$$\left[A_{ij}(\phi), B_{ij}(\phi)\right] = \int_0^{\phi} \left(a_{ij}(\phi), b_{ij}(\phi)\right) d\phi \qquad \text{(A5k)}$$

For small to moderate values of ϕ, it is possible to use the following representations for the losses in various stiffnesses in (A5f-k) and (A5m) to match test data for in-situ softening observed in $(\pm\theta)_{ns}$ and other laminate layups.

$$\begin{aligned} A_{11}(\phi) \pm B_{11}(\phi) &= C_{11}\left[1-\left(1+\phi/\phi_1^{\pm}\right)^{-n_1^{\pm}}\right] \\ 2A_{22}(\phi) = A_{22}(\phi) + B_{22}(\phi) &= k\left[1-\left(1+\phi/\phi_2^{+}\right)^{-n_2^{+}}\right] \\ A_{44}(\phi) &= G_T\left[1-\left(1+\phi/\phi_4\right)^{-n_4}\right] \\ A_{66}(\phi) &= G_A\left[1-\left(1+\phi/\phi_6\right)^{-n_6}\right] \end{aligned} \qquad \text{(A6a-d)}$$

It may be noted that these representations are adequate when the stress-strain relations are of the power law type after the onset of damage. Also, (A6b) and (A5h) imply that the material behaves elastically under hydrostatic compressive stress, i.e. $\sigma_2 = \sigma_3 = p$. These assumptions may not be adequate for large values of ϕ. From test data for AS4/3501-6 laminates reported in literature, it appears that the following parameters should yield reasonable fits to the laminate responses when ϕ is not large.

$$\begin{aligned} n_1^{+} &= 2.576, & \phi_1^{+} &= 4812\ in\ lb/in^3 \\ n_1^{-} &= 1.372, & \phi_1^{-} &= 2810\ in\ lb/in^3 \\ n_2^{+} &= 2.538, & \phi_2^{+} &= 22.68\ in\ lb/in^3 \\ n_4 &= 0.287, & \phi_4 &= 11.40\ in\ lb/in^3 \\ n_6 &= 0.478, & \phi_6 &= 14.86\ in\ lb/in^3 \end{aligned}$$

DAMAGE SURFACES FOR AN ISOTROPIC MATERIAL

In addition to the unidirectional fiber composites in wavy forms, textile composites contain matrix pockets, which are also brittle and will undergo stiffness loss with increasing strain. The Helmholtz free energy for such materials is chosen in the following simple form based on the principles of damage me-

chanics and assumptions similar to those used for the damage surfaces (in the previous sub-section) for fiber composites.

$$\rho\psi = \frac{1}{2}\left[K\varepsilon_v^2 + G\gamma_{eff}^2\right] - \int_o^{\phi} R(\underline{\varepsilon},\phi)d\phi$$
$$\gamma_{eff}^2 = 2\left(\varepsilon_{11}'^2 + \varepsilon_{22}'^2 + \varepsilon_{33}'^2\right) + \gamma_{12}^2 + \gamma_{23}^2 + \gamma_{13}^2 \qquad \text{(A7a,b)}$$

where K is the bulk modulus, G is the shear modulus.

$$\varepsilon_{\mathrm{v}} = \varepsilon_{11} + \varepsilon_{22} + \varepsilon_{33}, \text{ volumetric strain}$$
$$\varepsilon_{\mathrm{ij}}' = \varepsilon_{\mathrm{ij}} - \varepsilon_{\mathrm{v}}/3; (\mathrm{i} = \mathrm{j}), \text{ deviatoric strains} \qquad \text{(A7c-e)}$$
$$\gamma_{\mathrm{ij}} = \text{shear strains}; (\mathrm{i} \neq \mathrm{j})$$

$$\mathrm{R}(\underline{\varepsilon},\phi) = 1 \text{ (for damage growth to occur)} \qquad \text{(A7f)}$$

(A7f) define the damage surfaces for various values of ϕ and no damage growth will occur if $\mathrm{R}(\underline{\varepsilon},\phi) < 1$.

The simplest form of $\mathrm{R}(\underline{\varepsilon},\phi)$, which may be chosen is of the following form

$$\mathrm{R}(\underline{\varepsilon},\phi) = \frac{1}{2}\left[\left(\mathrm{a_v}(\phi) + \mathrm{b_v}(\phi)\operatorname{sgn}\varepsilon_{\mathrm{v}}\right)\varepsilon_{\mathrm{v}}^2 + \mathrm{a_s}(\phi)\gamma_{\mathrm{eff}}^2\right.$$
$$\left.\int_0^{\phi} \mathrm{R}(\varepsilon,\phi)\mathrm{d}\phi = \frac{1}{2}\left[\left(\mathrm{A_v}(\phi) + \mathrm{B_v}(\phi)\operatorname{sgn}\varepsilon_{\mathrm{v}}\right)\varepsilon_{\mathrm{v}}^2 + \mathrm{A_s}(\phi)\gamma_{\mathrm{eff}}^2\right]\right. \qquad \text{(A8a,b)}$$

Substitution of (A8b) in (A7a) and use of (A7g-i) yield the following expressions for stresses

$$\sigma_{\mathrm{ij}} = \left\{\mathrm{K} - \left(\mathrm{A_v}(\phi) + \mathrm{B_v}(\phi)\operatorname{sgn}\varepsilon_{\mathrm{v}}\right) - \frac{2}{3}\left(\mathrm{G} - \mathrm{A_s}(\phi)\right)\right\}\varepsilon_{\mathrm{v}}\delta_{\mathrm{ij}}$$
$$+ 2\left(\mathrm{G} - \mathrm{A_s}(\phi)\right)\varepsilon_{\mathrm{ij}}; \mathrm{i} = \mathrm{j} \qquad \text{(A8c,d)}$$
$$\tau_{\mathrm{ij}} = \left\{\mathrm{G} - \mathrm{A_s}(\phi)\right\}\gamma_{\mathrm{ij}}; \mathrm{i} \neq \mathrm{j}$$

It is clear that the damaged material behaves as an isotropic material with a reduced bulk modulus of $\left\{K - \left(A_v(\phi) \pm B_v(\phi)\operatorname{sgn}\varepsilon_v\right)\right\}$ and a reduced shear modulus of $\left\{\mathrm{G} - \mathrm{A_s}(\phi)\right\}$. If the material is assumed to behave elastically under hydrostatic compression then one may choose $B_V(\phi) = A_V(\phi)$. Power law type relations, similar to those discussed in the previous sub-section can again be chosen for A_V and A_S.

Note: The constitutive laws described above are used in the UMAT subroutine as described in the text. As evident from the average stress-strain plots of the fabric composites, the values of dissipated energies are not too large as compared to the stored energy (maximum values are of the order of 20%). It should be pointed out that when dissipated energies become large, the materials may no longer behave in transversely isotropic or isotropic fashion [17]. For the types of problems under consideration, however, the simple representations given here appear to be adequate.

The parameters needed for modeling stiffness losses (as in (A6b-d)) for unidirectional composites are obtained from stress-strain responses of unidirectional or laminated composites determined from standard coupon type tests. Parameters in (A6a) are chosen for an assumed softening pattern in the fiber direction. Ideally, they should be determined from tests on a laminate coupon with a hole. Parameters in (A8c,d) are obtained from tension, compression and shear tests on bulk epoxy material.

Table 1
Material properties of the yarns

Material	E_{11} ***GPa (Msi)***	E_{22} ***GPa (Msi)***	ν_{12}	ν_{23}	G_{12} ***GPa (Msi)***	G_{23} ***GPa (Msi)***
AS4/Epoxy 3501 (V_f^y = 0.64) [3]	144.80 (21.0)	11.73 (1.70)	0.230	0.30	5.52 (0.8)	3.3 (0.47)
E-Glass/Epoxy (V_f^y =0.65) [9]	48.47 (7.03)	18.06 (2.62)	0.25	0.34	5.58 (0.81)	3.31 (0.48)
AS4-Carbon/Epoxy 3501 (V_f^y = 0.70) [8]	155.83 (22.60)	10.13 (1.47)	0.24	0.5	5.72 (0.83)	3.38 (0.49)
Carbon/Epoxy (V_f^y = 0.6) [6]	135.27 (19.61)	9.65 (1.40)	0.28	0.43	5.37 (0.78)	3.38 (0.49)
Epoxy 3502 [8]	3.79 (0.55)	3.79 (0.55)	0.35	0.35	1.38 (0.20)	1.38 (0.20)

Table 2
Comparison of present results with analytical and experimental studies

Textile		E_x ***GPa (Msi)***	E_z ***GPa (Msi)***	ν_{xy}	ν_{zx}	G_{xy} ***GPa (Msi)***	G_{xz} ***GPa (Msi)***
AS4/Epoxy Plain weave (V_f^o = 0.64)	Present	62.33 (9.04)	11.84 (1.72)	0.060	0.420	4.7125 (0.68)	3.85 (0.56)
	Experimental [3]	61.92 (8.98)	-	0.110	-	-	-
	FEA [3]	63.78 (9.25)	11.38 (1.65)	0.031	0.329	4.82 (0.69)	4.97 (0.72)
AS4/Epoxy 5-harness satin (V_f^o = 0.64)	Present	66.09 (9.58)	11.75 (1.70)	0.050	0.410	4.17 (0.60)	3.85 (0.56)
	Experimental [3]	69.43 (10.06)	-	0.060	-	5.24 (0.76)	-
	FEA [3]	65.99 (9.57)	11.38 (1.65)	0.030	0.320	4.96 (0.72)	5.03 (0.73)
AS4/Epoxy 8-harness satin (V_f^o = 0.64)	Present	66.99 (9.71)	11.57 (1.67)	0.045	0.37	4.462 (0.65)	3.99 (0.57)
	Experimental [3]	72.19 (10.47)	-	0.06	-	6.76 (0.98)	-
	FEA [3]	66.74 (9.68)	11.45 (1.66)	0.03	0.32	4.96 (0.72)	5.03 (0.73)

Table 3
Geometrical Properties of Yarns

Material	Yarn width mm (in.)	Yarn thickness mm (in.)	Yarn spacing mm (in.)	V_f^y	V_f^o
E-Glass/epoxy [9]	1.747 (0.068)	0.268 (0.010)	1.747 (0.068)	0.65	0.35
AS4-Carbon/epoxy [8]	1.760 (0.069)	0.129 (0.005)	1.760 (0.069)	0.70	0.60
Carbon/epoxy [6]	2.499 (0.0984)	0.109 (0.0043)	2.499 (0.0984)	0.63	0.50